



Lab experience: the microfabrication process of electro-optical devices, while attempting to achieve high doping level in a silicon substrate.

Author: ALESSANDRO ANDREA VOGRIG, MATTEO ROSSETTO, XIAOHUI XU

Professors: ANDREA IVANO MELLONI, ANDREA SCACCABAROZZI

Academic year: 2021-2022

1. Introduction

Silicon doping is a fundamental part of many microfabrication processes. In the telecommunication world, for example, electro-optical modulators depend on the possibility of doping the material that composes them, forming the junction that enables their function. For these reasons it is extremely useful to be able to master in-house doping processes. During this Lab Experience at Polifab, the feasibility of this process has been proven using dopant sources developed in the laboratory itself, maintaining cost effectiveness, low toxicity, and simplicity as requirements. For these reasons, inorganic acids such as boric acid and phosphoric acid have been used as dopant sources, initially in conjunction with easily available low toxicity solvents, then in a silicon oxide sol gel formulation. The methods used were spin coating and thermal diffusion doping due to their simplicity, an essential factor for a good replicability of what was obtained.

This activity also offered the precious opportunity to follow the development process of microelectronic and electro-optical devices at a didactic level, starting from the CAD drawing and reaching the end of the physical realization process. Optical ring modulators, diodes of various sizes, a resistor and N-mosfet transistor have been made. The didactic aspect of the process was privileged with respect to the design according to the state of the art.

The following paragraphs describe the manufacturing process at a procedural level, indicating each time our considerations derived from the various tests. Finally, the conclusions regarding the results we have obtained will be presented.

2. Preliminary phase

2.1. Surface resistivity measurement in virgin samples

In the early stages of the laboratory activities, the silicon was characterized before any subsequent process was carried out. The wafers used were divided into 2cm-square samples. The samples have a thickness of $525\mu\text{m}$ and are slightly P doped. The surface resistivity was measured using a 4-point probe sys-

tem. This system measures the potential difference detected between two test leads, while a current is flowing through two other adjacent test leads, allowing for precise measurements, avoiding the influence of contact resistance. The data sheet of the wafers we used indicates a surface resistivity value between $100\Omega/\square$ and $300\Omega/\square$. We measured around $170\Omega/\square$ resistivity from the samples of the first wafer. It is worth mentioning that a good difference in surface resistivity between one wafer and another can be present; for example, an average difference of $50\Omega/\square$ was found between two wafers from the same batch we used. Therefore, it is important to obtain a reference measurement for each new wafer used in order to verify the success of the doping procedure with greater accuracy.

	Meas. 1	Meas. 2	Avg	Err
S. 1	169,36	170,42	169,89	0,44%
S. 2	169,7	170,93	170,31	0,51%
S. 3	169,82	172,53	171,17	1,12%

Table 1: Surface resistivity values of the silicon used in Ω/\square @ $100\ \mu\text{A}$

The relation between surface resistivity and doping level is a well-known characteristic in silicon. Thus, it is possible to derive the level of diffused atoms from the measured resistivity. Low resistivity values are indicative of higher doping.

2.2. Spin coating

Using a spincoater dopant solutions were deposited. A solution of 5%v/v boric acid diluted in acetone and a solution of 5%v/v phosphoric acid diluted in acetone were used. Before conducting the actual diffusion process, the samples were dried on a hot plate at 200°C . During this step, the poor wetting properties of the dopants in the acetone solution became immediately evident as large stains of dopant solution were visible spread over the sample. To mitigate this effect, the samples were cleaned of dopant, passed through a plasma cleaning cycle and recoated with dopant, obtaining better results.

2.3. Baking

The samples were baked in a tube furnace with a nitrogen atmosphere in pairs (one sample with phosphorus and one with boron), performing three different bakes at different temperatures to verify the variations in the diffusion profile. The nitrogen atmosphere was used to limit the formation of surface oxides during the process.

	Temp	Time
Batch 1	1100°C	2h
Batch 2	1050°C	2h
Batch 3	1000°C	2h

Table 2: Temperatures and baking time

2.4. Post processing and result review

Once the baking process is complete, it is necessary to remove the oxide (silicon oxide) present on the surface, which would otherwise affect the validity of subsequent measurements. Oxide stripping can easily be performed using hydrofluoric acid or, as in our case, BOE solution. This operation is called wet etching, as it uses liquid substances to achieve the desired result. The process involves placing the samples in a Petri dish containing the reagent for a specific period of time. The complete removal of the oxide can be easily determined by observing the surface of the sample, which must acquire a silvery colour and become hydrophobic. The subsequent resistivity tests using the 4-probe system revealed the situation shown in table 3.

	Avg	Err
P1 - 1100°C	64,28	76,06%
P2 - 1050°C	59,15	42,75%
P3 - 1000°C	25,07	45,00%

Table 3: Surface resistivity in Ω/\square after oxide removal

Several conclusions can be drawn from the data obtained. It is possible to affirm that the diffusion process actually took place. This is shown by the decrease in surface resistivity. It is also possible to notice a very high error due to the poor characteristics of the dopant solutions used, which did not uniformly wet the sample during the spin-coating process. For this reason, dopant solution with acetone as diluent were substituted with new solution based on a silicon oxide sol-gel. Another important consideration that emerges from the data is an opposite trend to what is expected in dopant diffusion: in fact, at higher temperatures the dopant concentration in the substrate should increase, whereas the experimental results show a decrease. This behavior has no certain explanation, but can be justified in various ways. A first hypothesis is related to the dopants used: excessive concentrations of boric acid

and phosphoric acid in the dopant solution and so on the samples during the baking stage could have caused an alloy to form with the silicon, altering its properties. Another hypothesis involves some form of unidentified chemical contamination or the formation of secondary reaction by-products in the dopant solutions during the baking process. Attempting to achieve better results, it was decided to further clean the samples by growing an oxide layer that would incorporate the impurities and later be removed. This procedure partially improved the results but still revealed a lack of uniformity.

	Avg	Err
P1 - 1100°C	51,20	50,91%
P2 - 1050°C	26,64	7,44%
P3 - 1000°C	15,22	15,17%
B1 - 1100°C	12,14	23,33%
B2 - 1050°C	36,91	9,88%
B3 - 1000°C	165,30	2,67%

Table 4: Surface resistivity in Ω/\square after cleaning

2.5. Test with silicon oxide sol-gel

As mentioned earlier, the final samples containing the optical modulators were made with a new type of doping solution called sol-gel, capable of ensuring better uniformity. As with previous doping solutions, test samples were also made, with promising results in terms of uniformity and level of doping achieved.

	Avg	Err
P-1100°C	3,14	2,85%
P-1000°C	11,34	1,48%
P-900°C	69,52	0,95%
B-1100°C	4,14	1,34%
B-1000°C	72,28	1,21%
B-900°C	159,02	0,36%

Table 5: Surface resistivity in Ω/\square with new dopant solution

3. Fabrication of a resistor

Before adopting the new dopant solutions, two resistors were fabricated with the solution with acetone, one with phosphorus dopant and the other one with boron dopant. These resistors proved useful in establishing the consistency of the process.

3.1. Litography e diffusion

The samples were coated with an oxide layer using a PECVD machine and then covered with an AZ5214E photoresist film. Positive lithography was then carried out using an MLA100, a machine with an ultra-violet laser capable of exposing the sample without the need for an exposure mask. After the exposure step, the photoresist was developed by immersing the sample in AZ726MIF developing solution for about

1 minute. The samples were then hard baked at 150°C for 10 minutes in order to harden the photoresist and make it resistant to hydrofluoric acid attack. Indeed, the idea is to remove the oxide layer in correspondence of the resistor template, so that the dopant can diffuse into the silicon substrate and the remaining oxide acts as a screen against diffusion into unwanted areas. The success of the etching step was verified via a profilometer. Finally, the actual diffusion stage was performed by coating the samples with boric and phosphoric acid dopants in acetone solution. The samples were then baked for 2 hours at 950°C.

3.2. Result review

On a first look under an optical microscope the samples were visibly deteriorated with several surface stains, especially in N-type ones. The removal of the surface oxide layer formed in the furnace slightly improved the appearance of the samples.

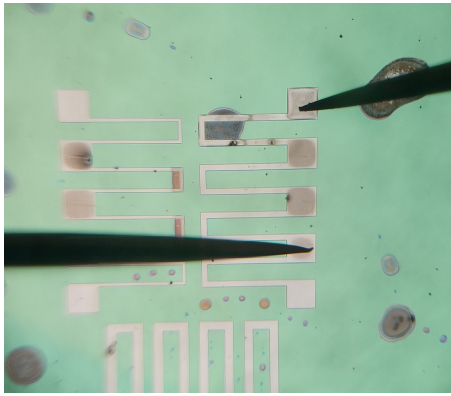


Figure 1: Resistors at probing station

The resistors obtained were tested at the probing station to trace their I/V curve and extrapolate their resistance. From the resistance curves in function of resistors length, it can be seen that the intercept doesn't cross the zero: this is an expected result. Indeed, the contact zones have not been covered with a layer of metal and there is, therefore, a contact resistance of approximately 2,5 ohms. The results obtained indicate good uniformity for all phosphorus resistors, in fact as the length of the resistive tract increases linearly, the measured resistance increases linearly too. The presence of stains of dubious composition has, in some cases, compromised the functionality of the resistor, acting as an insulator and interrupting the resistive material path. However, different conclusions are obtained for boron resistors. In this case, contact resistance is dominant so the intrinsic resistance values obtained are too noisy and therefore invalid. This effect could be justified by the different diffusion profile of this dopant compared to the phosphoric one.

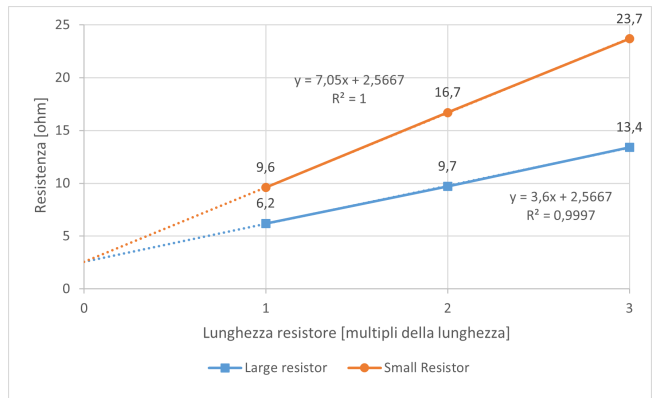


Figure 2: Resistors linearity. Resistance vs length

4. Mircoelectronic and electro-optical devices

After observing the results achieved with the resistors, it was decided to proceed with the employment of the new doping solution, capable of mitigating the problems encountered. The final samples consisted of a series of microelectronic and electro-optical devices. The primary objective was to verify the ability of these devices to be realised with the diffusion process just tested.

4.1. Design and project choices

The designed devices consist of: two resistors, obtained from two N+ doped zones; diodes with different junction sizes ($80\mu\text{m}$, $50\mu\text{m}$ e $20\mu\text{m}$); twenty-two N-Fets of various sizes; six ring modulators, with resonance centred around a wavelength of $6\mu\text{m}$. The area used is one square centimetre. The choice of a $6\mu\text{m}$ resonator wavelength, which is little used in telecommunications, is due to the technical limitations of the machinery used for lithographic exposure.

4.2. Physical realization

The lithography and diffusion process are carried out similarly as what done for the resistor. Since both dopants must be diffused in the same sample, the process has to be repeated twice taking care to align the design details with the aid of markers. At first, before starting the diffusion processes, the waveguide was etched together with the markers. In order to etch the guide, the Bosch process was performed in a dry etching machine (in this case, the term dry etching indicates the absence of liquid reagents, since gases are used). The entire substrate was eroded, apart from the areas protected by the photoresist, which then form the guide. The profile of the guide was verified by profilometry and by measurement under an electron microscope.

Although etching the guide prior to the doping steps may seem counterintuitive as it creates perturbations in the substrate surface that may affect the spinning process, it was verified that the non-doped silicon's uniformity guarantees better and more homogeneous

etching results.

Finally, a metal layer was deposited by evaporation to create contacts and oxidation with silicon oxide was let it happen. The metal used was copper, bonded to silicon through a layer of chromium, which act as a bounder. It is important to point out that the deposition of the copper contacts must necessarily be the last step in the process because heating a silicon sample containing copper would irreparably damage it, due to copper's tendency to diffuse in the crystal lattice creating short circuits.

4.3. Analysis of the results

The analysis of the manufactured samples was carried out both morphologically, using an optical and an electron microscope, and electrically, at the probing station. The analysis was not limited to the finished sample, but was conducted throughout the entire fabrication process, in order to verify step by step the correct execution of each stage.

The first important check we conducted was verifying the separation between the coupled waveguides, initially with an optical microscope and then with an electron microscope.

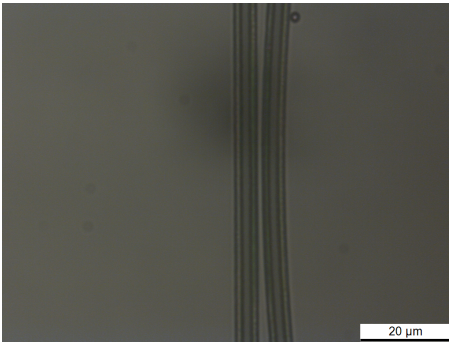


Figure 3: Waveguide coupling - Optical microscope
The image under the optical microscope also shows how the walls of the waveguide are not perfectly vertical. This is due to the photoresist profile used. Using an electron microscope, it was possible to observe the waveguide surface (figure 4). By observing the image, it is possible to hypothesize that the losses in the structure are quite high: the imperfections accumulated in the lithographic process and, above all, during the dry etching, have generated a fairly irregular surface and, presumably, with a high scattering during operation.

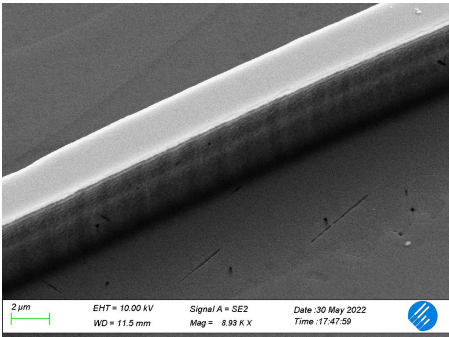


Figure 4: Waveguide profile

Thanks to the different conductivity of the various zones, that are modified by the dopants presents, it was possible to observe the diffusion of the different dopings to the electron microscope (figure 5). Alignment markers are visible at the corners; the T-shaped metal contacts are very bright due to the material they are made of; the phosphorus-doped N+ zone is clearly visible on the left. The boron-doped P+ zone can be spotted on the right. In addition, the details of this image allow us to study the lateral diffusion of the dopant at a qualitative level: by design the P and N zones were spaced 2 μ m apart, whereas physically this spacing has disappeared.

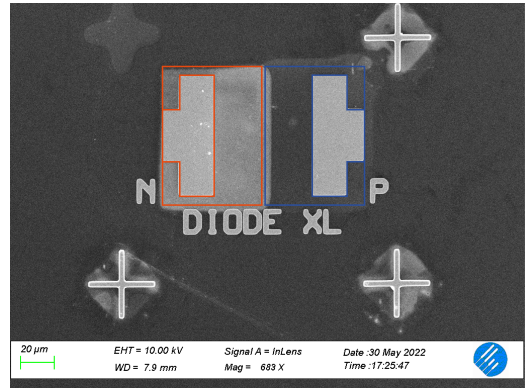


Figure 5: N well (red perimeter) and P well (blue perimeter) at a junction

The yield was less than 100%, due to the thin waveguides that were lost in some modulators. However, the junctions were found to be functional.

Tests of the electrical characteristics were carried out at the probing station, performing a voltage sweep and recording the current delivered. The graph in figure 6 provides a comparison of the I/V curves of the resistors present in two different samples. From the plot it is possible to exclude, for the tested range, the formation of junctions as the curves are perfectly linear. The comparison of the curves of the two resistors allows us to conclude that the consistency of diffusion is maintained well across different samples.

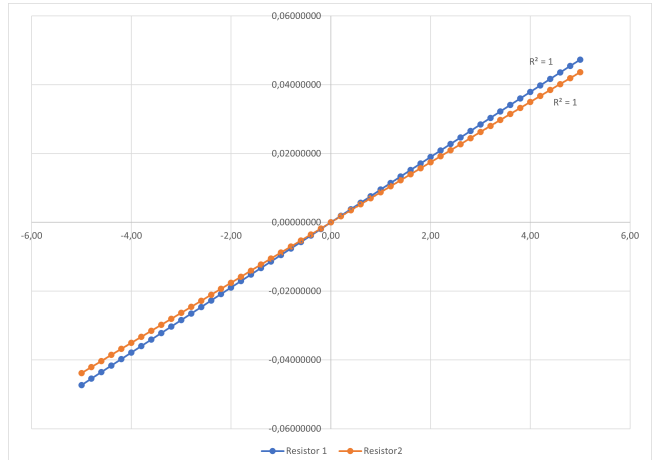


Figure 6: I/V curves in the resistors of two samples
The junction present in the resonator is of the PIN

type, given the non-doped layer that makes up the guide rib. Even if an exhaustive test was not done (switching times and parasitic capacitances were not measured), the I/V curve is characteristic of a diode showing a conduction voltage around 1V and a reverse breakdown voltage of about -7V.

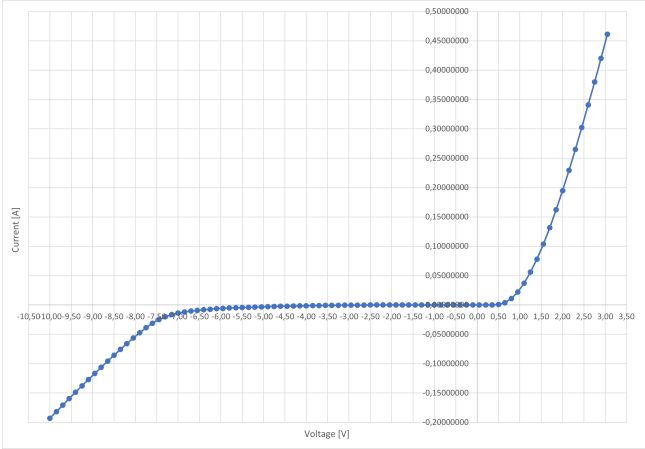


Figure 7: I/V curve of the diode in the modulator

A finer analysis allows us to identify some conductivity, though only 1mA around 0.5V is measured. The leakage current remains between $0.8\mu\text{A}$ and $15\mu\text{A}$, values comparable with some commercial-grade diodes. During the diode measurements, an attempt was made to maintain a semi-darkness environment to avoid photoelectric effects. As a final test, however, a measurement of one of the smaller diodes was made in both darkness and full light, using the microscope illuminator as the source. Because of the photoelectric effect, the curve in the inversion zone is clearly altered.

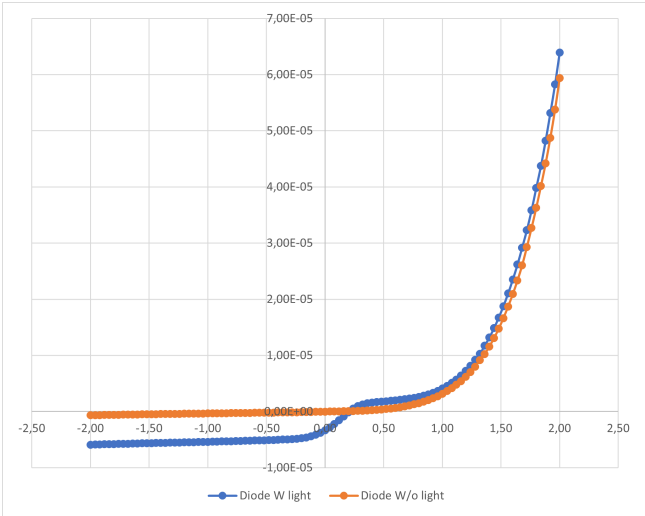


Figure 8: Comparison of I/V curves between illuminated and darkened diode

5. Conclusions

Although the yield of our samples was not 100%, as expected for a process still in a development phase, and the resonators were not optically tested, we can nonetheless conclude that we have successfully

achieved our goals. Indeed, in addition to the physical realisation of the design, the doping process by means of diffusion was successfully verified. The PN junctions of the diodes and PIN junctions of the optical modulators showed the typical curve present in the diodes, the resistors were linear. Furthermore, the doped samples showed good uniformity overall. However, the refinement of the diffusion process is not yet complete: as our Lab Experience comes to an end, studies to optimise the dopant solution, to precisely define the diffusion curves and to establish the effects of ageing on the samples and dopants are still activities that need to be pursued in the future.

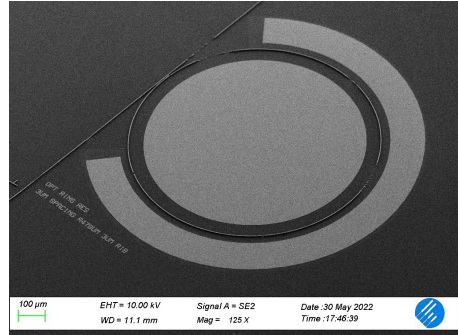


Figure 9: Full optical modulator